

Supporting Information

Computational Determination of Potential Inhibitors of SARS-CoV-2 Main Protease

Son Tung Ngo,^{ab} Ngoc Quynh Anh Pham,^c Ly Thi Le,^d Duc-Hung Pham,^{e*} and Van V. Vu,^{f*}*

^aLaboratory of Theoretical and Computational Biophysics, Ton Duc Thang University, Ho Chi Minh City 700000, Vietnam

^bFaculty of Applied Sciences, Ton Duc Thang University, Ho Chi Minh City 700000, Vietnam

^cHo Chi Minh University of Technology, Ho Chi Minh City 700000, Vietnam

^dSchool of Biotechnology, International University, Ho Chi Minh City 700000, Vietnam

^eDivision of Immunobiology, Cincinnati Children's Hospital Medical Center, Cincinnati 45229, OH, USA

^fNTT Hi-Tech Institute, Nguyen Tat Thanh University, Ho Chi Minh City 700000, Vietnam

*Email: ngosontung@tdtu.edu.vn; duchung.pham@cchmc.org; and vanvu@ntt.edu.vn

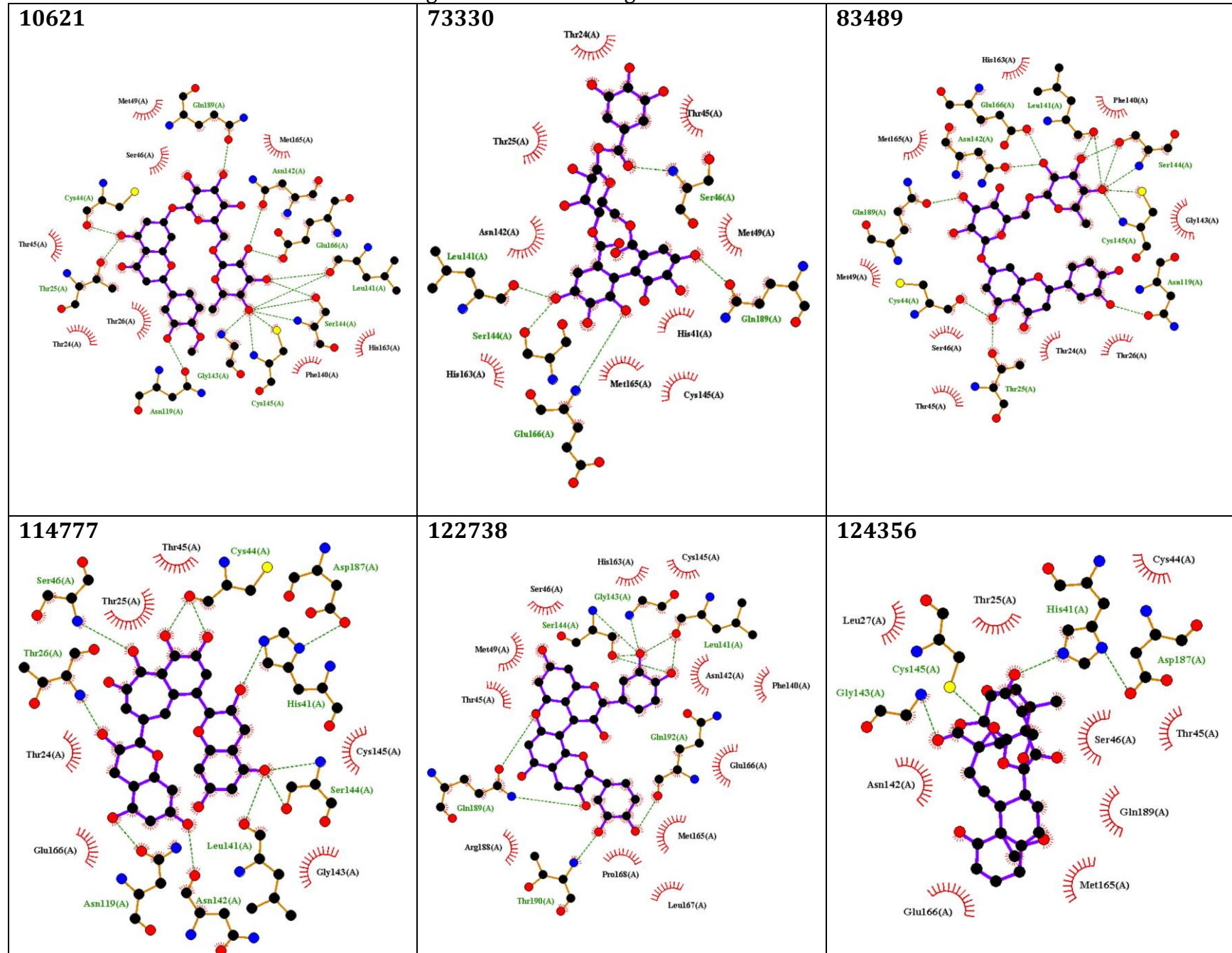
Table S1. The List of Top-Lead Compounds forming a Large Affinity Obtained via Molecular Docking Simulations.^a

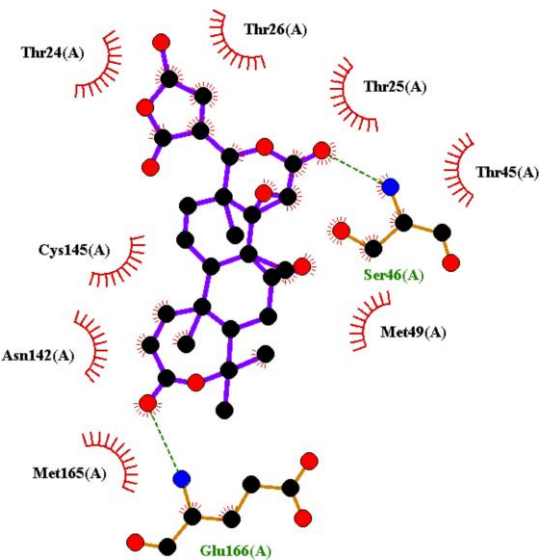
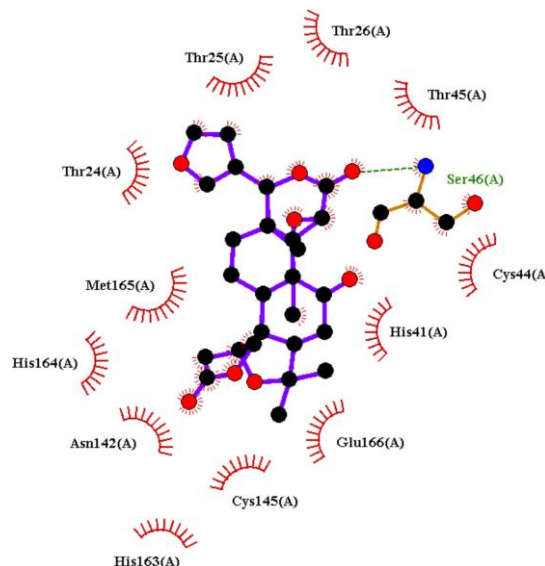
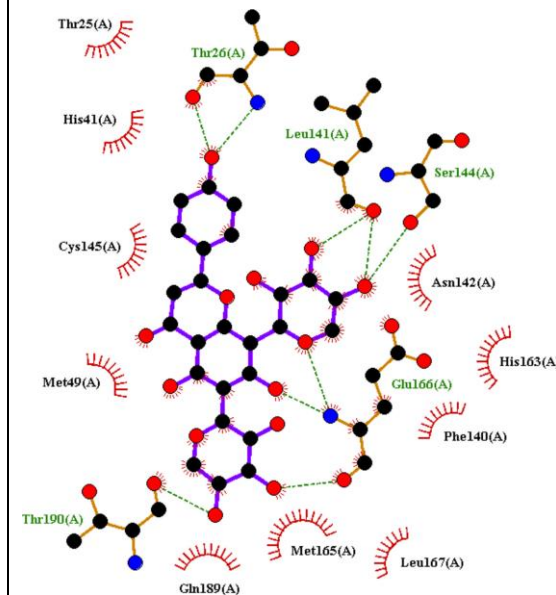
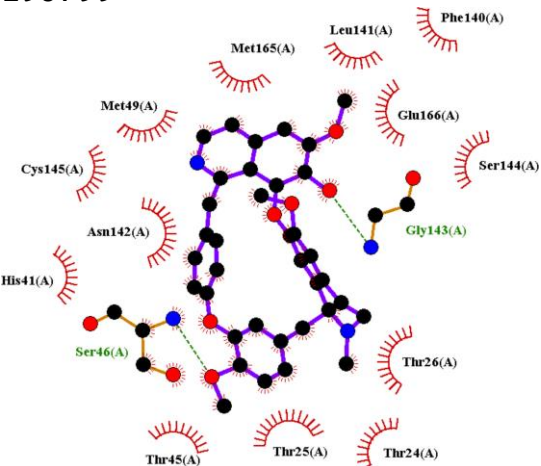
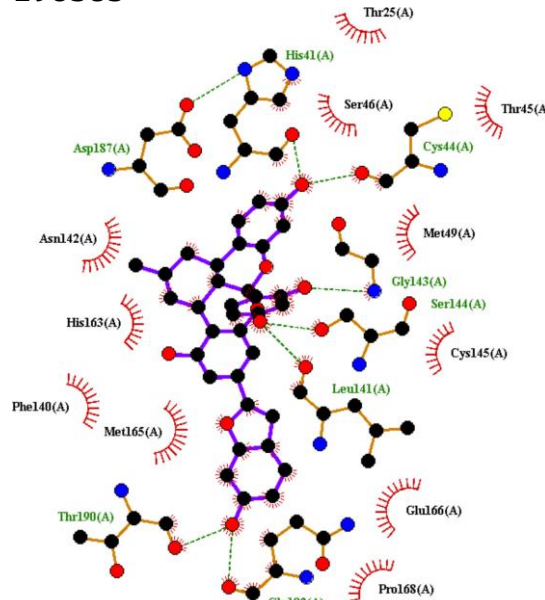
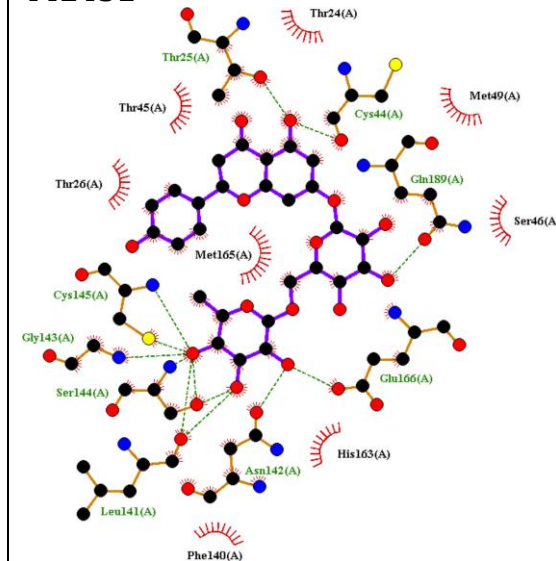
Nº	Pubchem	Compound Name	Vietnamese Herb Name	ΔG_{Dock}
1	10621	Hesperidin	Citrus Aurantium	-9.0
2	73330	Strictinin	Castanea Molissima/ Juglans Regia/ Psidium Guajava	-8.7
3	83489	Eriocitrin	Mentha Piperita	-9.1
4	114777	CHEMBL346119	Camellia Sinensis	-8.7
5	122738	Procyanidin B2	Cinnamomum Cassia	-8.6
6	124356	Physalin F	Physalis Angulata	-8.9
7	156766	Kihadanin B	Phelodendron Amurens	-8.6
8	179651	Limonin	Citrus Aurantium/ Coptis Chinensis/ Phelodendron Amurens/ Citrus Reticulata	-9.0
9	183905	6,8-Di-C-Beta-D-Arabinopyranosyl Apigenin	Camellia Sinensis	-8.7
10	190799	Stephasubine	Stephania Hernandifolia	-9.2
11	196583	Mulberrofuran G	Morus Alba	-9.3
12	442431	Narirutin	Citrus Aurantium/ Cynara Scolymus/ Citrus Sinensis	-8.9
13	480819	Albanol B	Morus Alba	-9.1
14	5281600	Amentoflavone	Garcinia Xanthochymus	-8.6
15	5281613	Diosmin	Pratia Nummularia	-9.1
16	5281627	Hinokiflavone	Rhus Succedanea/ Cycas Revoluta/ Cupressus Funnebris	-8.6
17	5317025	Linarin	Mentha Aquatica	-9.1
18	5319276	Marchantin K	Marchantia Polymorpha	-9.0
19	5319278	Marchantin L	Marchantia Polymorpha	-8.7
20	5319933	Mulberrofuran Q	Morus Alba	-8.6
21	5458744	Physalin B 5,6-Epoxide	Physalis Angulata	-8.7
22	6476333	Isoacteoside	Fernandoa Adenophylla/ Stereospermum Cylindricum/ Clerodendrum Inerme/ Markhamia Stipulata/ Rehmannia Glutinosa/ Plantago Asiatica/	-8.8

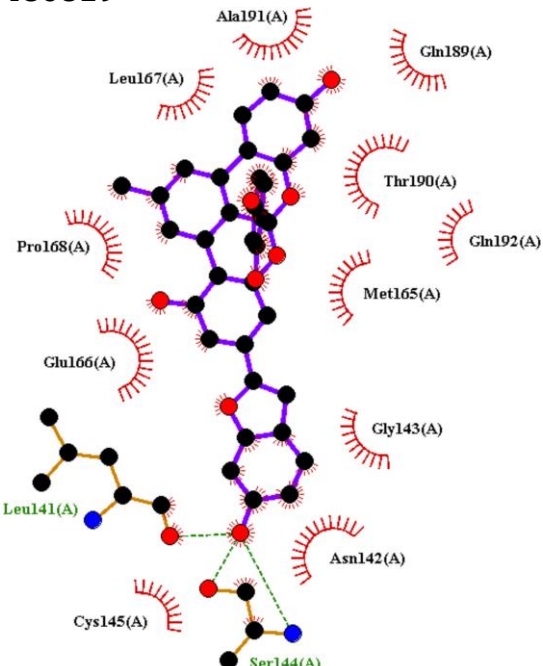
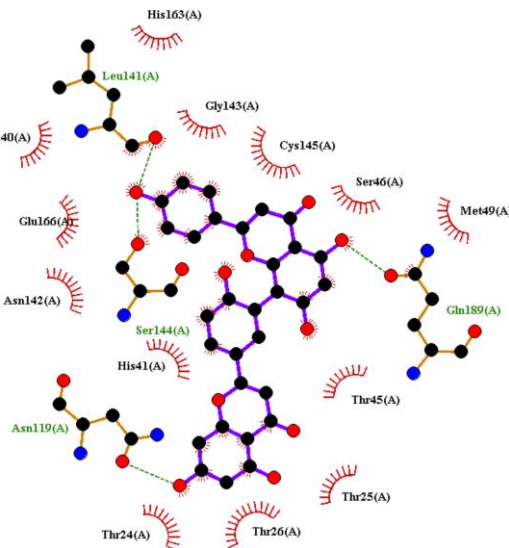
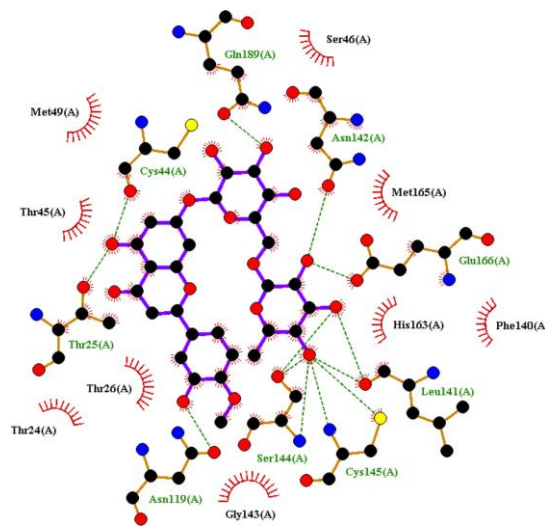
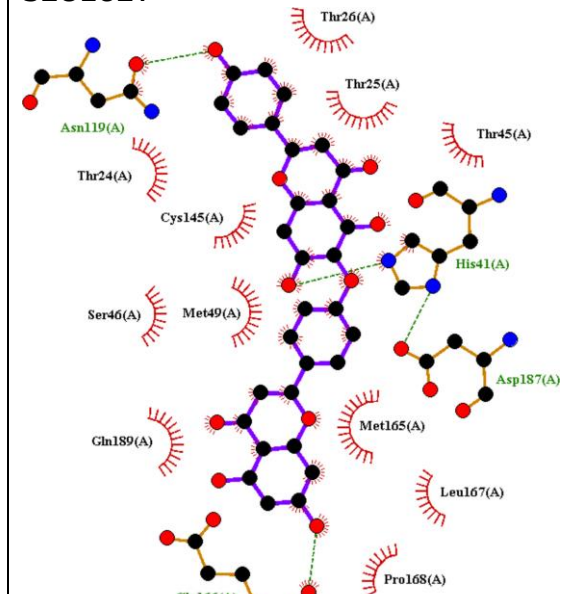
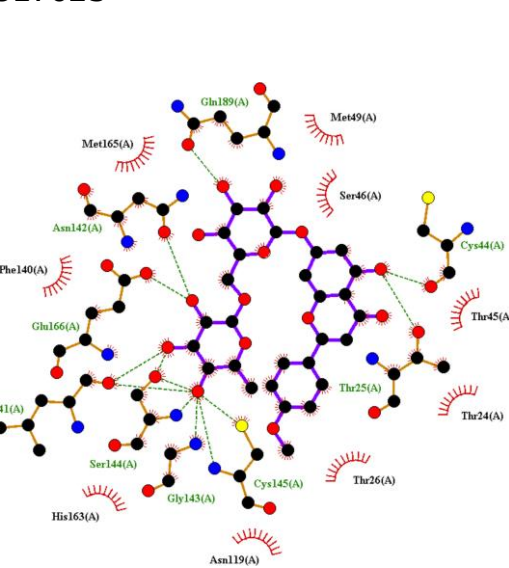
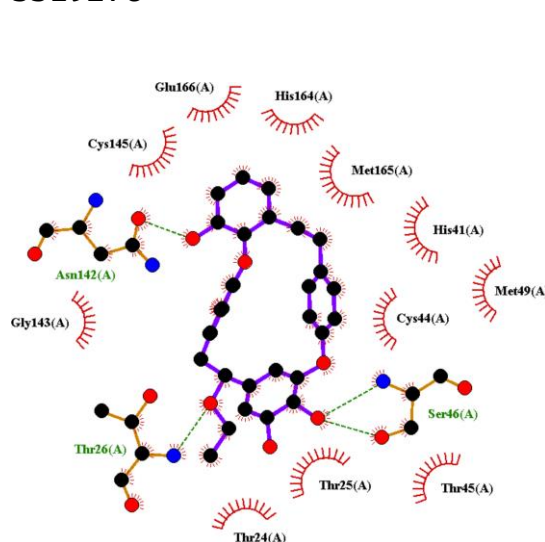
			Acanthus Ebracteatus	
23	6711179	Hypopistephanine	Stephania Japonica	-9.8
24	9851181	Isorhoifolin	Mentha Aquatica/ Citrus Paradisi/ Pratia Nummularia	-9.0
25	10456516	Cinchonain-Ib	Kandelia Candel	-8.6
26	10461109	Luteolin-7-O-Beta-Rutinoside	Capsella Bursa/ Mentha Aquatica/ Pratia Nummularia	-9.2
27	11827970	Diosgenin Glucoside	Borassus Flabellifer	-9.3
28	15086398	Cannabisin A	Cannabis Sativa	-8.8
29	16760075	Didymin	Citrus Sinensis	-9.0
30	21123844	Gamma-Chaconine	Solanum Tuberosum	-8.9
31	44558930	Anabsinthin	Artemisia Absinthium	-9.0
32	71437113	2,3-Dihydrohinokiflavone	Cycas Revoluta	-8.8
33	71448965	Cannabisin D	Cannabis Sativa	-8.6
34	90473381	(1 <i>R</i> ,2 <i>S</i> ,5 <i>S</i> ,8 <i>S</i> ,9 <i>R</i> ,14 <i>R</i> ,15 <i>R</i> ,17 <i>R</i> ,18 <i>R</i> ,21 <i>S</i> ,24 <i>R</i> ,26 <i>R</i> ,27 <i>S</i>)-5,14,15-Trihydroxy-2,9,26-Trimethyl-3,19,23,28-Tetraoxaoctacyclo[16.9.1.1 ^{18,27} .0 ^{1,5} .0 ^{2,24} .0 ^{8,17} .0 ^{9,14} .0 ^{21,26}]Nonacos-11-Ene-4,10,22,29-Tetron	Physalis Angulata/ Physalis Minima	-9.1
35	101764560	Quercetin-7-O-Rutinoside	Platycodon Grandiflorum	-9.2
36	65016	Amprenavir		-6.6
37	148192	Atazanavir		-6.6
38		Aza-Peptide Epoxide		-6.4
39	213039	Darunavir		-6.9
40	5362440	Indinavir		-7.6
41	92727	Lopinavir		-7.0
42	64143	Nelfinavir		-7.0
43	392622	Ritonavir		-6.5
44	441243	Saquinavir		-7.6

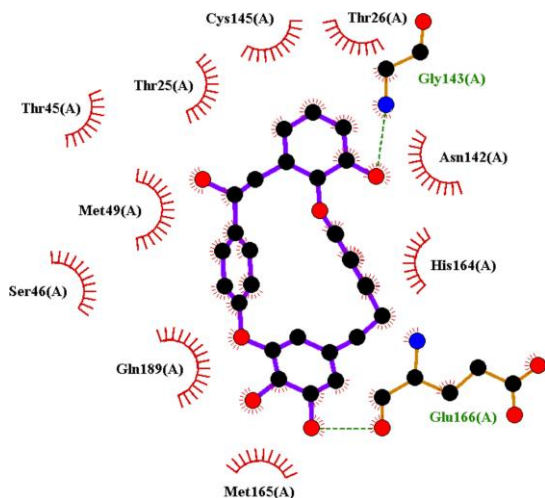
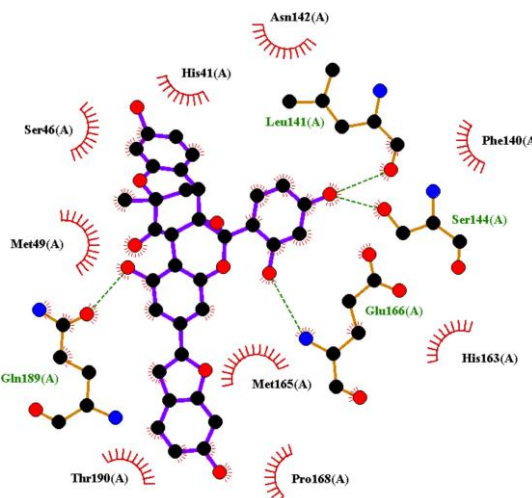
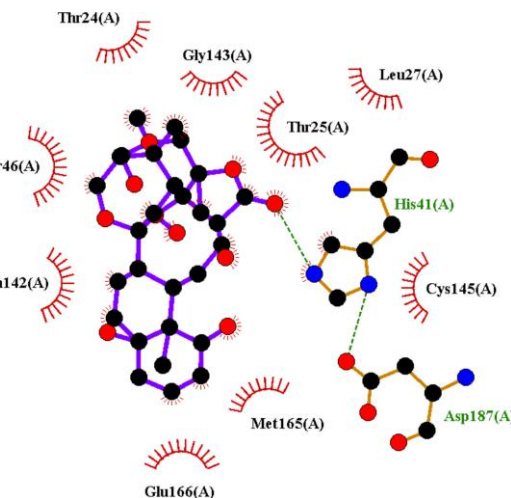
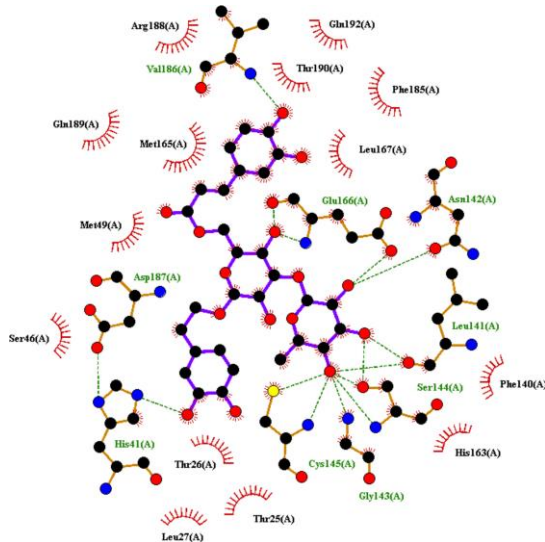
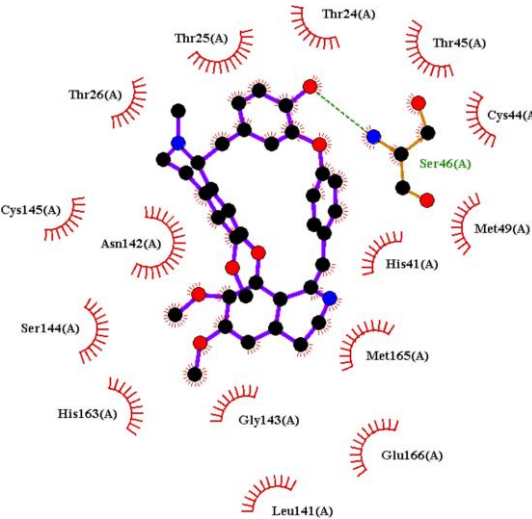
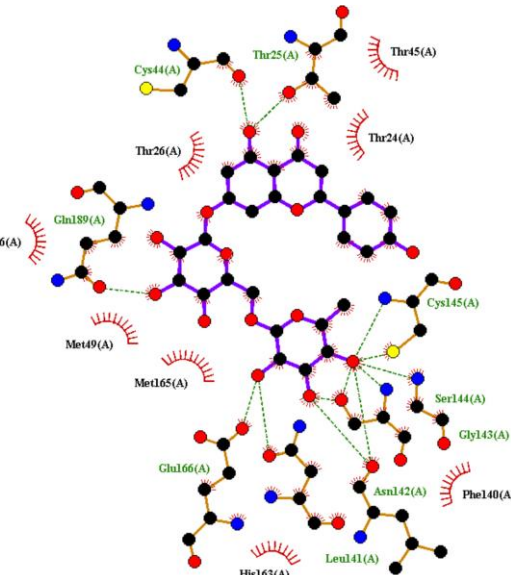
^aThe Docking Binding Free Energy Was Obtained by Autodock Vina. The Mean Rupture Force ΔF_{Max} and The Mean Pulling Work ΔW were Obtained from 8 Independent Trajectories of SMD Simulations. The Error is Standard Error of the Mean. The Unit of Energy/Work and Force are pN and kcal/mol, respectively.

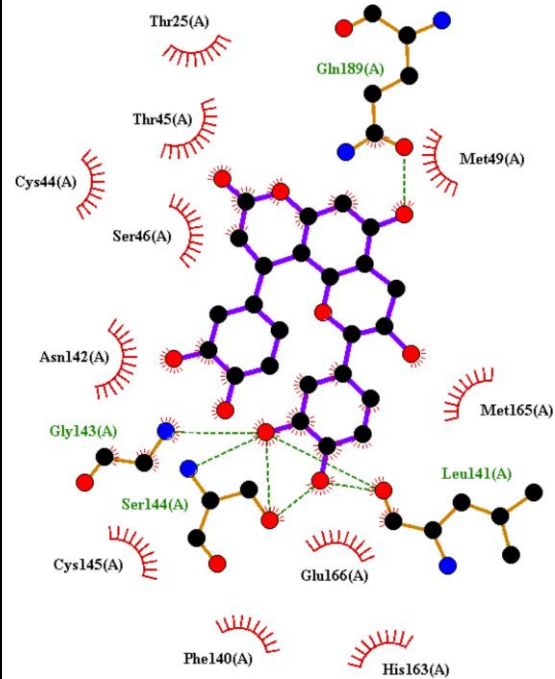
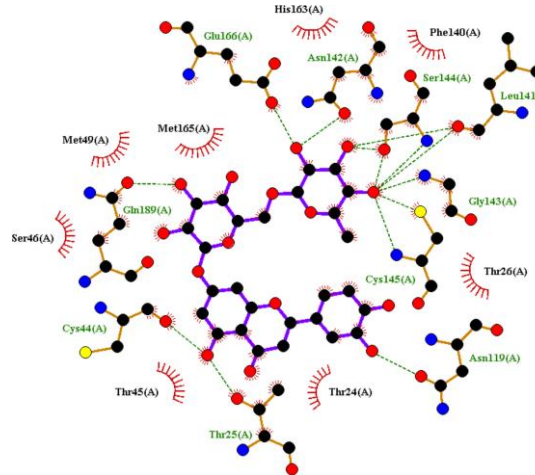
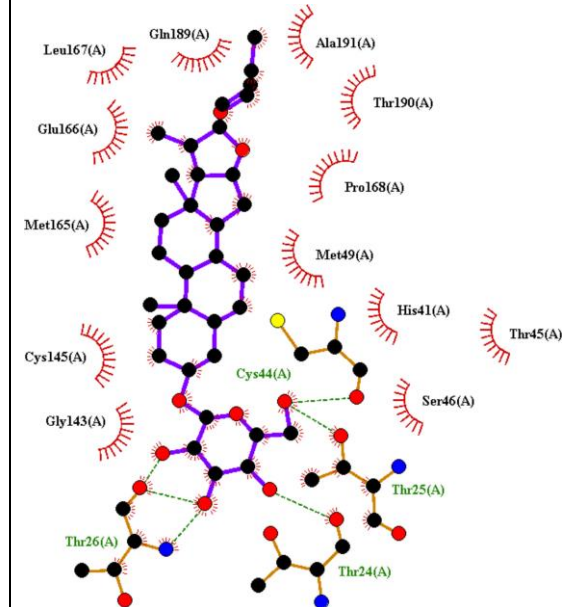
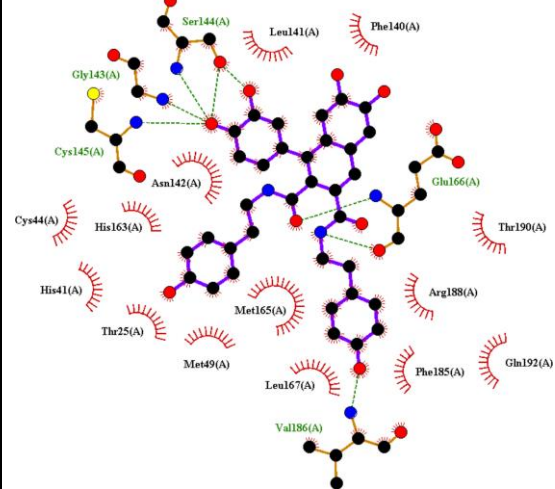
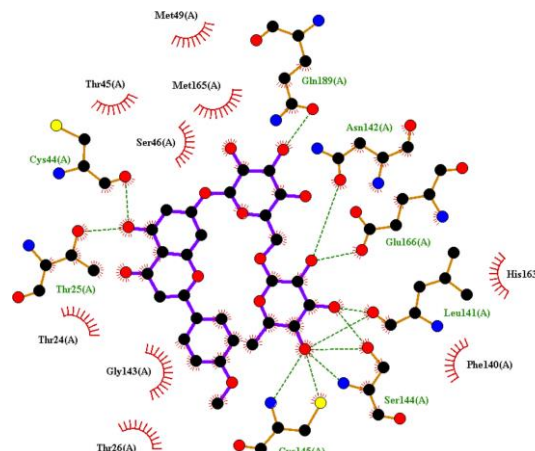
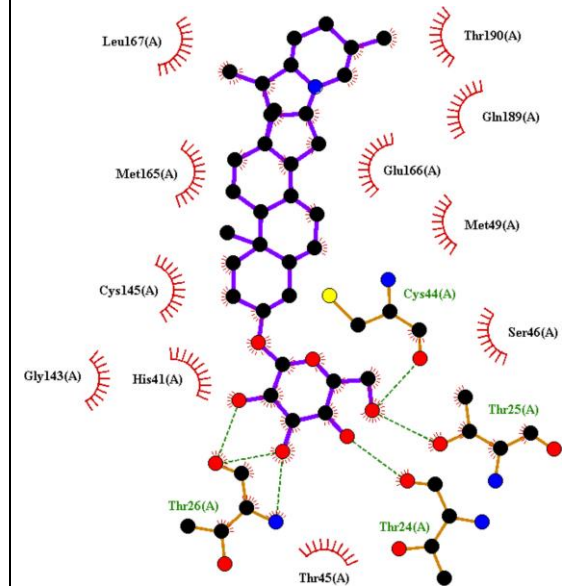
Table S2. The Two-Dimensional Protein-Ligand Interaction Diagrams.^a

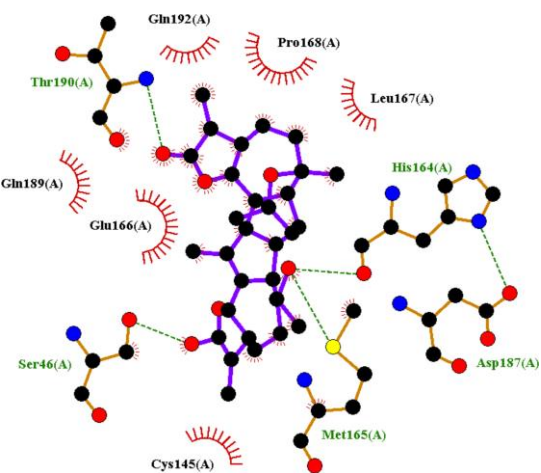
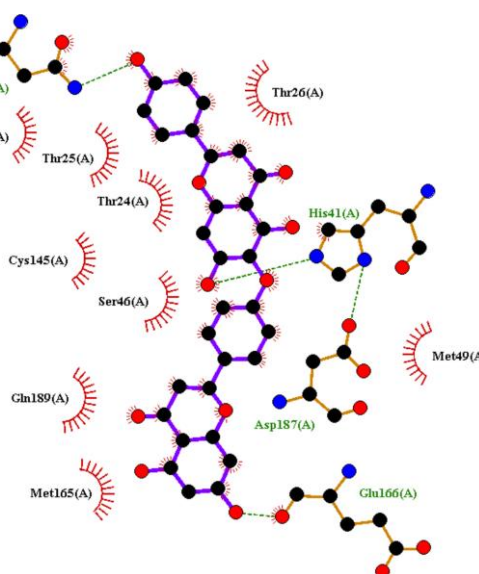
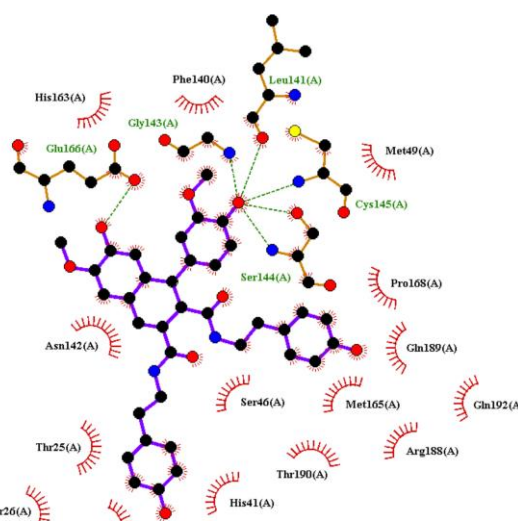
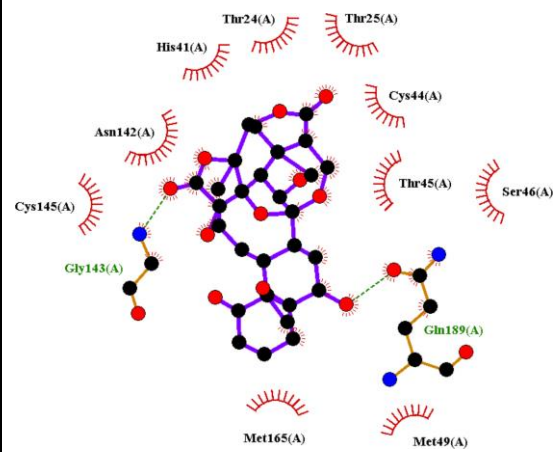
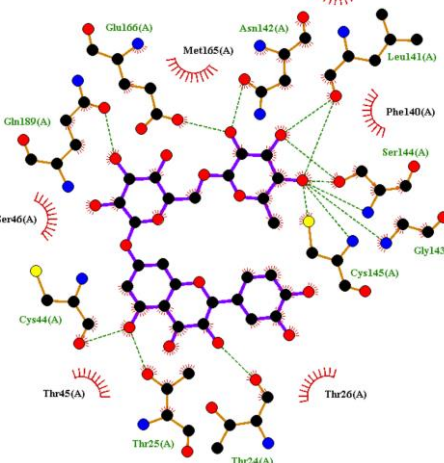
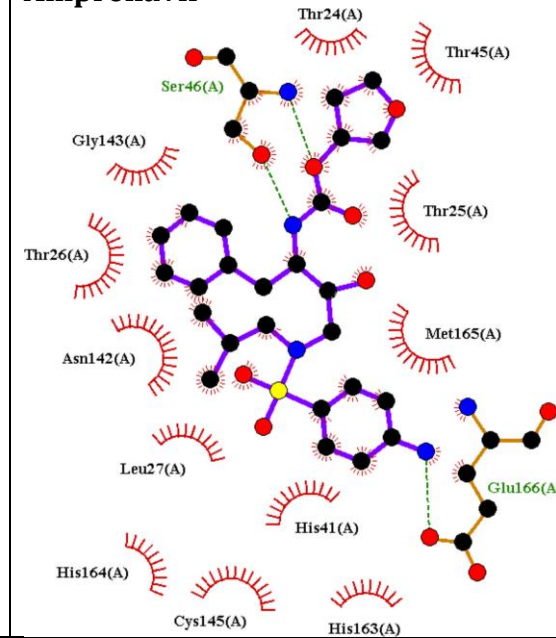


156766**179651****183905****190799****196583****442431**

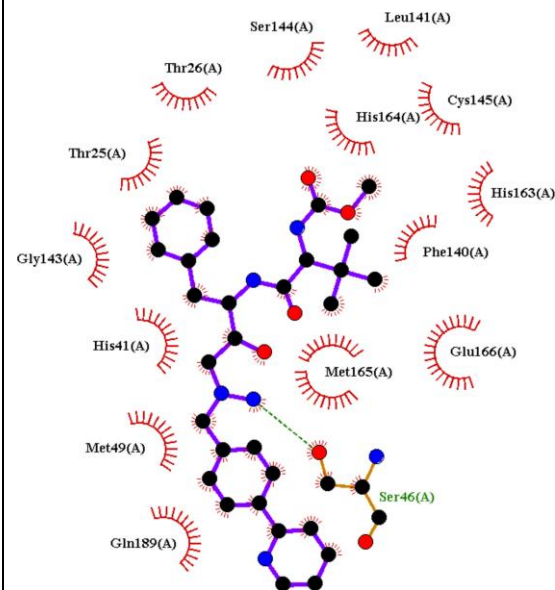
480819**5281600****5281613****5281627****5317025****5319276**

5319278**5319933****5458744****6476333****6711179****9851181**

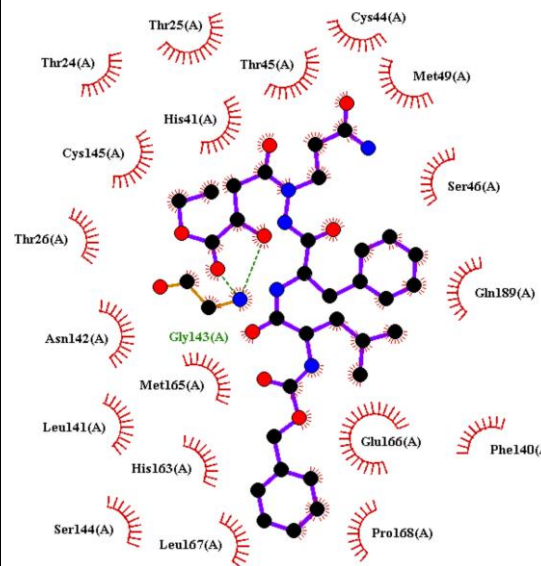
10456516**10461109****11827970****15086398****16760075****21123844**

44558930**71437113****71448965****90473381****101764560****Amprenavir**

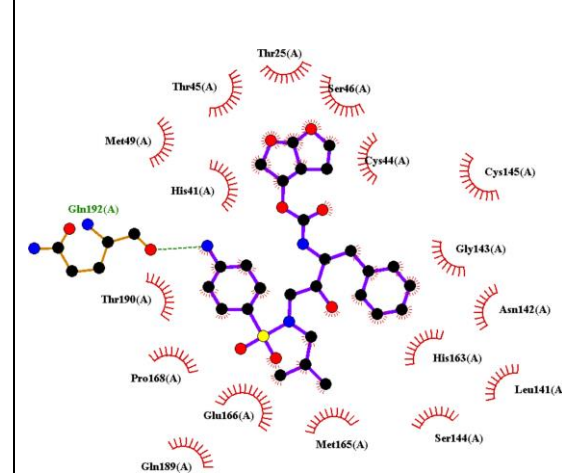
Atazanavir



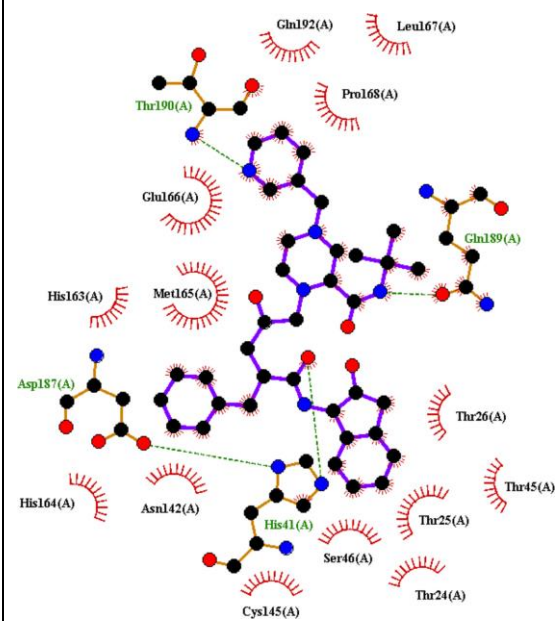
Aza-Peptide Epoxide



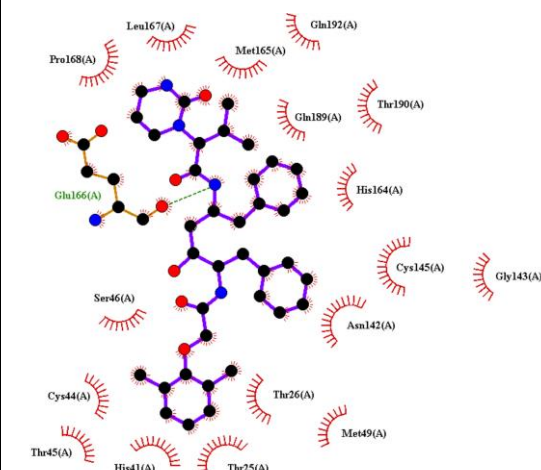
Darunavir



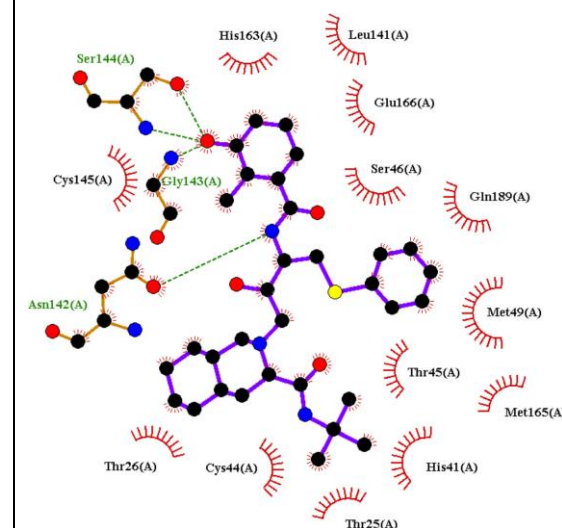
Indinavir



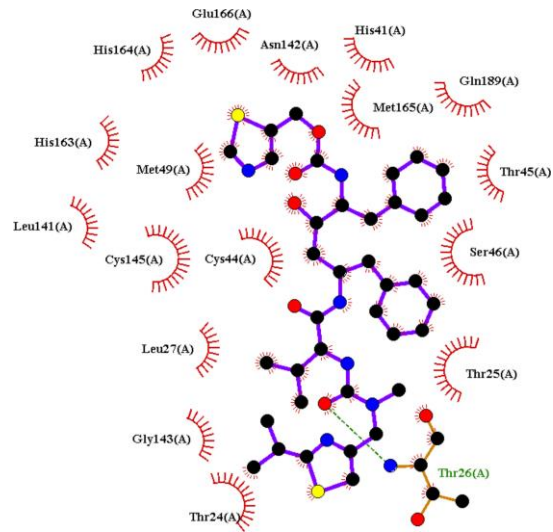
Lopinavir



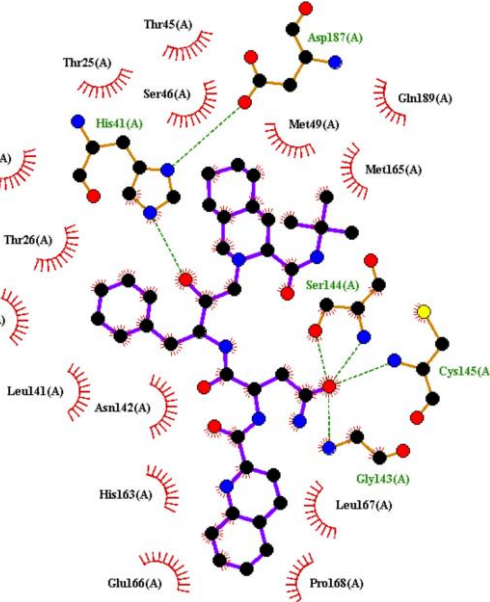
Nelfinavir



Ritonavir



Saquinavir



^aThe Obtained Results were Prepared via the LigPlot++ package.¹

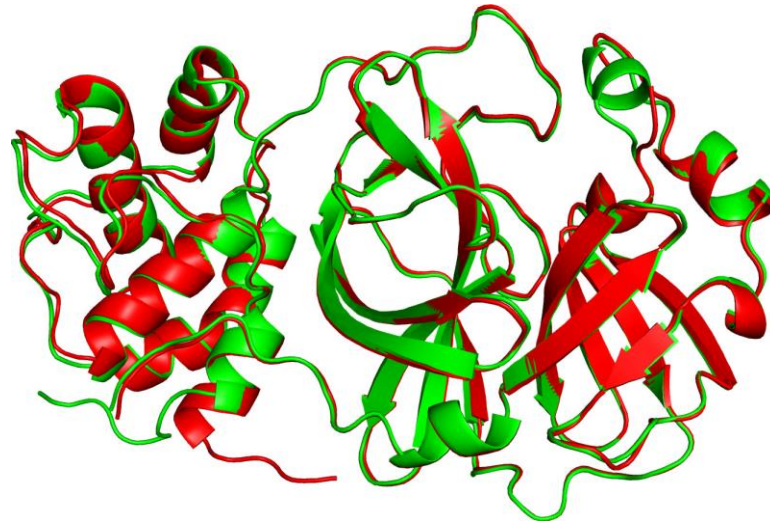


Figure S1. Super position between the modelled SARS-CoV-2 Mpro² and the experimental structure.³ The C_{α} RMSD between two structures is of 0.05 nm.

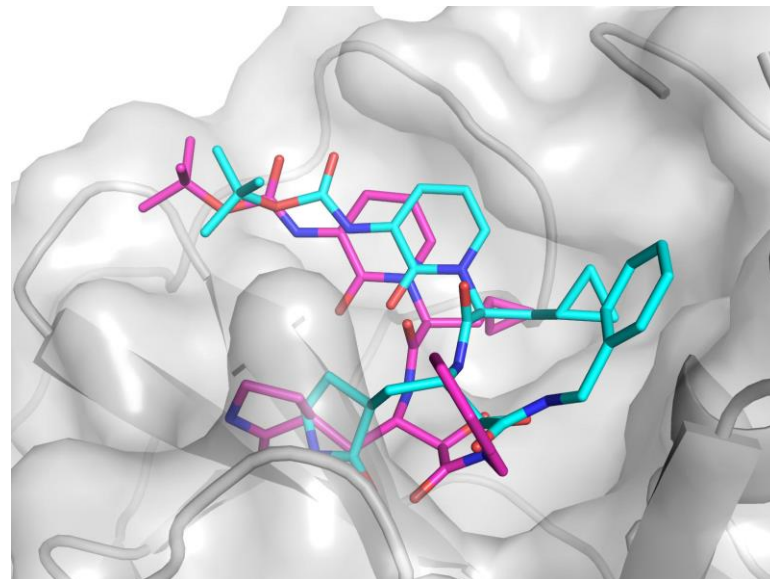
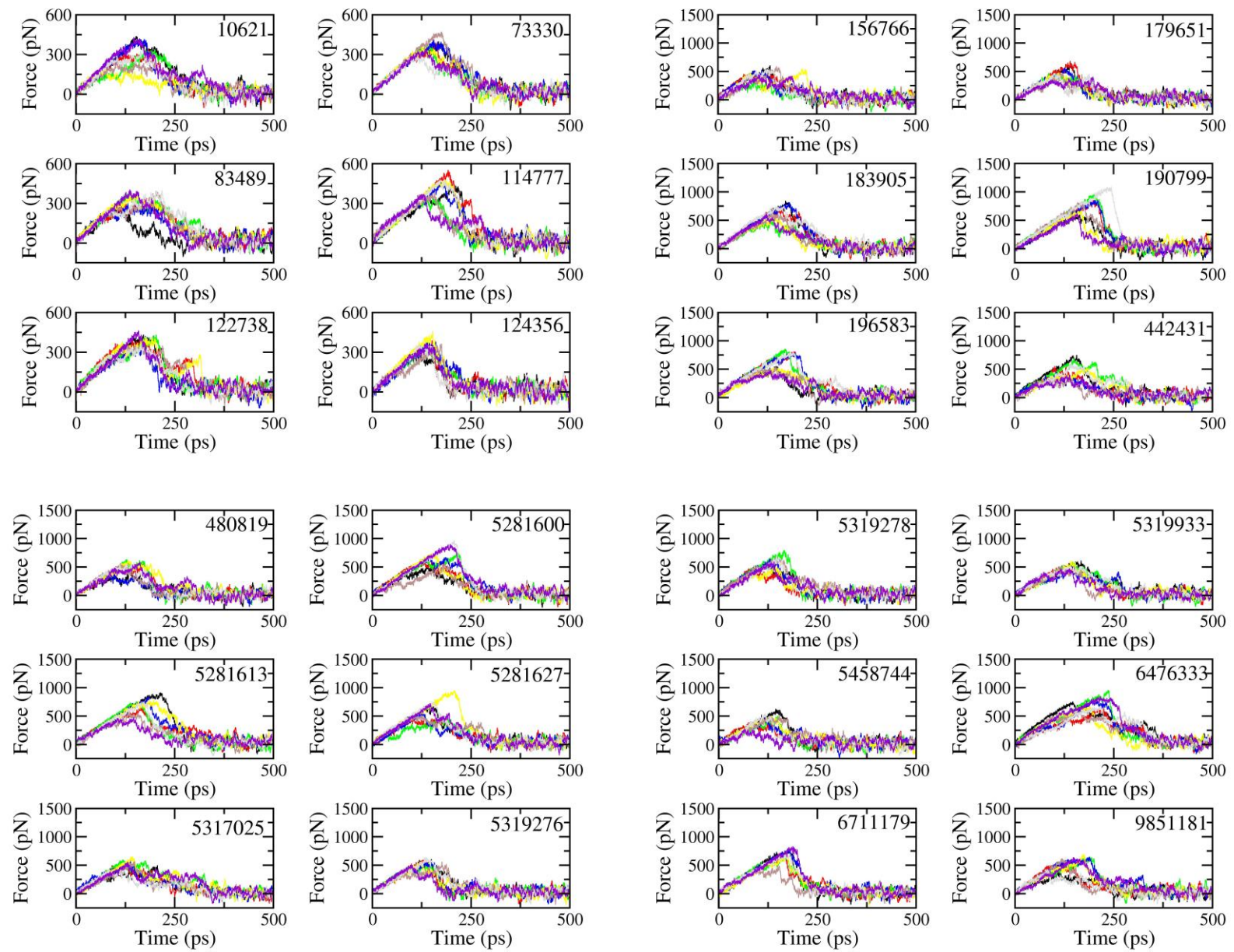


Figure S2. Super position between the experimental (purple)³ and computational (cyan) poses between compound **13b** and SARS-CoV-2 Mpro. The C_{α} RMSD between two structures is of 0.19 nm.



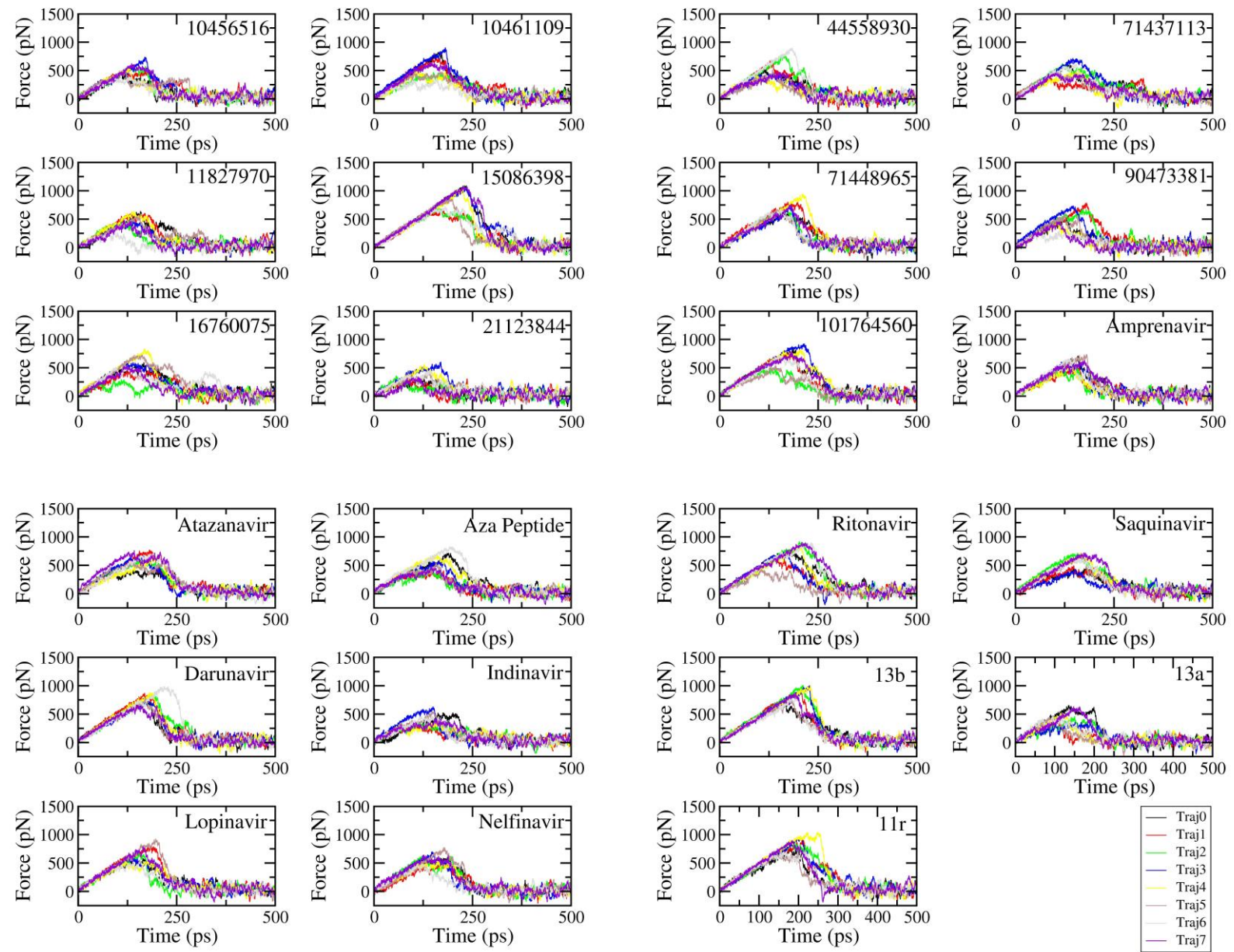


Figure S3. The pulling force in time dependence over 8 independent SMD trajectories.

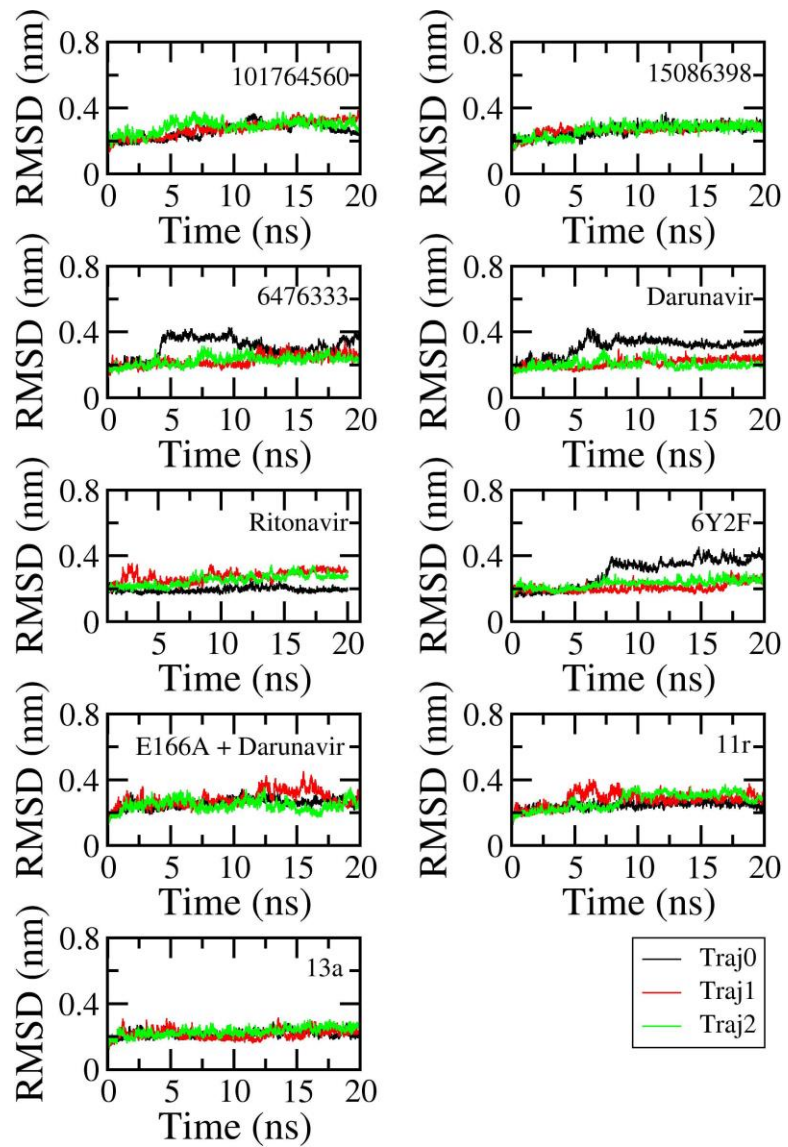


Figure S4. All-atoms RMSD of SARS-CoV-2 Mpro + Inhibitors over 3 independent MD simulations with length of 20 ns.

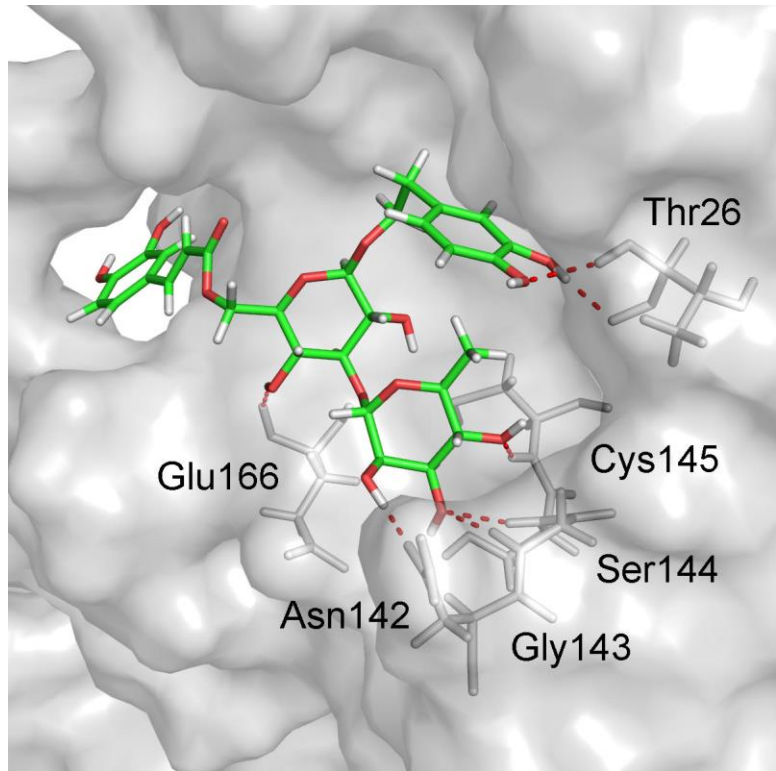


Figure S5. The binding pose of the SARS-CoV-2 PR + *isoacteoside* system. This result was obtained by all-atom clustering with a cutoff 0.3 nm using 3000 equilibrium snapshots.

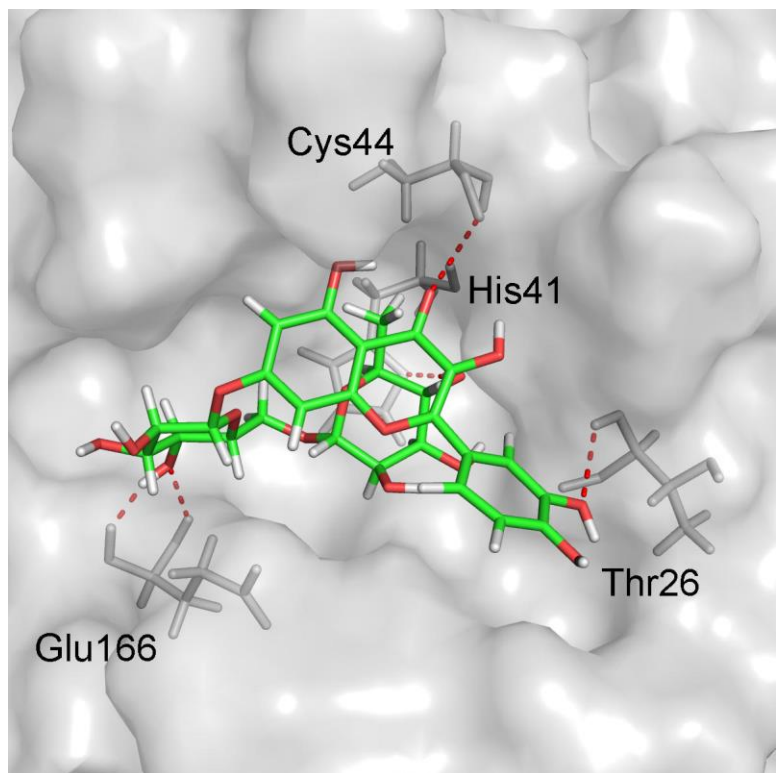


Figure S6. The binding pose of the SARS-CoV-2 PR + *quercetin 7-o-rutinoside* system. This result was obtained by all-atom clustering with a cutoff 0.3 nm using 3000 equilibrium snapshots.

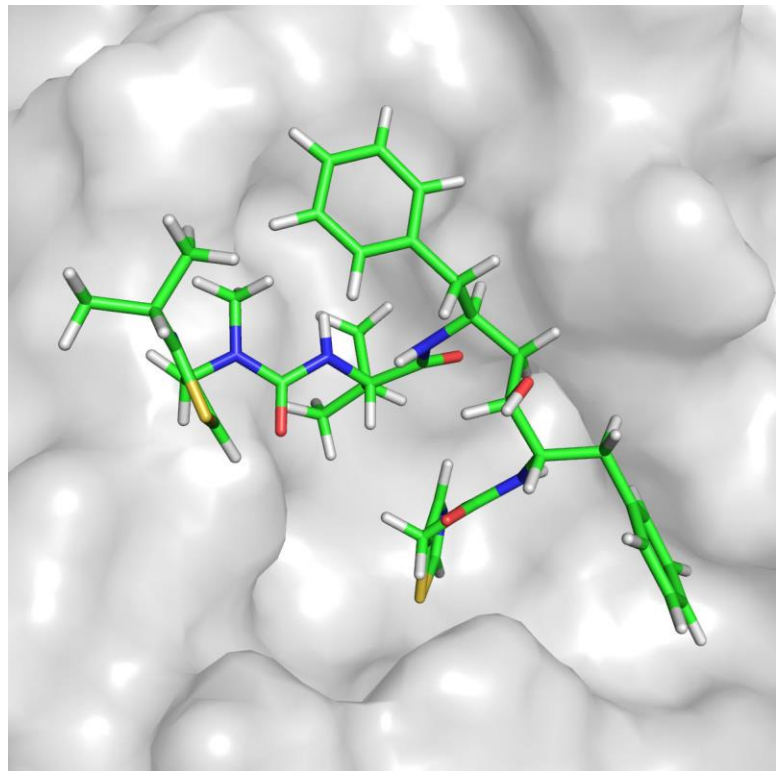


Figure S7. The binding pose of the SARS-CoV-2 PR + *ritonavir* system. This result was obtained by all-atom clustering with a cutoff 0.3 nm using 3000 equilibrium snapshots.

Video S1. The dynamics of SARS-CoV-2 Mpro + *cannabisin A* during MD simulations.

Reference:

1. Laskowski, R. A.; Swindells, M. B., LigPlot+: Multiple Ligand–Protein Interaction Diagrams for Drug Discovery. *J. Chem. Inf. Model.* **2011**, *51* (10), 2778-2786.
2. Christian C., G.; Georg, S. Wuhan coronavirus 2019-nCoV – what we can find out on a structural bioinformatics level 2020. https://figshare.com/articles/innophore-com-2019-ncov_2020-01-29_pdf/11752749.
3. Zhang, L.; Lin, D.; Sun, X.; Curth, U.; Drosten, C.; Sauerhering, L.; Becker, S.; Rox, K.; Hilgenfeld, R., Crystal Structure of SARS-CoV-2 Main Protease Provides a Basis for Design of Improved α -Ketoamide Inhibitors. *Science* **2020**, *368*, 409-412.